iScience

Article

Mechanosensitive interactions between Jag1 and Myo1c control Jag1 trafficking in endothelial cells

Graphical abstract

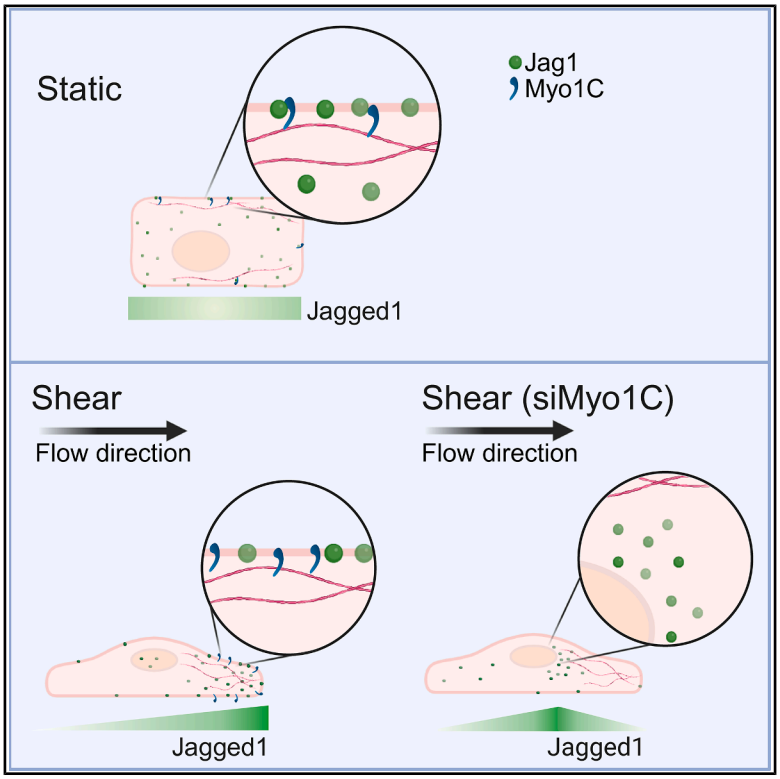

Highlights

- Fluid flow shear stress on endothelial cells polarizes Jag1 downstream of flow
- Myo1c interacts with Jag1, and shear stress reduces the interaction
- Knockdown of Myo1c reduces shear-induced polarization
- Under static conditions Myo1c knockdown reduces Jag1 levels at the membrane

Authors

Oscar M.J.A. Stassen, Noora Virtanen, Kai-Lan Lin, ..., Garry L. Corthals, Carlijn V.C. Bouten, Cecilia M. Sahlgren

Correspondence

cecilia.sahlgren@abo.fi

In brief

Mechanobiology; Biochemistry; Molecular interaction; Cell biology

Stassen et al., 2025, iScience *28*, 113879
December 19, 2025
https://doi.org/10.1016/j.isci.2025.113879

CellPress

iScience

CellPress
OPEN ACCESS

Article

Mechanosensitive interactions between Jag1 and Myo1c control Jag1 trafficking in endothelial cells

Oscar M.J.A. Stassen,[1,2,4,5] Noora Virtanen,[1,2,3,8] Kai-Lan Lin,[1,2,3,8] Freddy Suarez Rodriguez,[1,2,3] Matthijs J.M. Heijmans,[4] Feihu Zhao,[6] Garry L. Corthals,[7] Carlijn V.C. Bouten,[4,5] and Cecilia M. Sahlgren[1,2,3,4,5,9,*]

[1]Faculty of Science and Engineering, Cell Biology, Åbo Akademi University, Turku, Finland
[2]Turku Bioscience, Åbo Akademi University and University of Turku, Turku, Finland
[3]InFLAMES Research Flagship Center, Åbo Akademi University and University of Turku, Turku, Finland
[4]Department of Biomedical Engineering, Eindhoven University of Technology, Eindhoven, the Netherlands
[5]Institute for Complex Molecular Systems (ICMS), Eindhoven University of Technology, Eindhoven, the Netherlands
[6]Department of Biomedical Engineering, Zienkiewicz Institute for Modelling, Data & AI, Faculty of Science and Engineering, Swansea University, Swansea, UK
[7]Van 't Hoff Institute for Molecular Sciences (HIMS), University of Amsterdam, Amsterdam, the Netherlands
[8]These authors contributed equally
[9]Lead contact
*Correspondence: cecilia.sahlgren@abo.fi
https://doi.org/10.1016/j.isci.2025.113879

SUMMARY

Morphogenesis of the cardiovascular system is responsive to hemodynamic cues sensed by endothelial cells. The organization of morphogenic signaling proteins is regulated by membrane presentation and internalization. Here, we aimed to characterize factors that regulate this flow-dependent protein localization by identifying differential interactors with the Notch ligand Jagged1 in response to shear stress. We cultured endothelial cells expressing Jagged1-APEX2 for proximity labeling on an orbital shaker shear stress platform. Myo1c was identified and confirmed through coimmunoprecipitation as a Jagged1-interacting factor under static conditions, with reduced interaction after exposure to shear. Jagged1 polarization downstream of shear followed by nucleograde transport was inhibited by Myo1c knockout. Further, Myo1c knockdown reduced membrane levels of Jagged1 under static but not shear conditions. Together, our data reveal a role for Myo1c in the hemodynamic control of Jagged1 localization in endothelial cells.

INTRODUCTION

Surface membrane proteins play a central role in mediating cellular interactions and signaling. To control interactions, cells continuously refine the protein population at their surface through regulated protein trafficking.[1] The surface membrane protein Jagged1 (Jag1) is one of the ligands of the Notch receptor family and has important functions in the vasculature. Loss of Jag1 is embryonically lethal, and various congenital or acquired cardiovascular diseases are associated with Jag1 mutation or dysfunction, including atherosclerosis, Alagille syndrome, or tetralogy of Fallot.[2–5]

Notch is a highly regulated and dose-sensitive signaling pathway.[6] There are several mechanisms to control the dose of Notch activation, including post-translational modifications, control of membrane presentation, and combinatorial levels of ligands of varying affinity presented in *cis* or in *trans*,[7] but the mechanisms with which the cell controls trafficking of Jag1 are poorly understood.[8,9] In endothelial cells, Jag1 levels and their distribution within the endothelial network have been shown to be post-transcriptionally controlled by the ZFP36 mRNA decay protein,[10] and the activity of Jag1 in Notch signal activation is intricately linked to the mechanical state of the cardiovascular system.[5,11] Jag1 has been shown to have distinct molecular mechanical properties, possibly related to catch bond principles.[12] At the cellular level, Jag1 reorganizes under shear stress, which promotes its functionality as a signal sender in Notch signaling.[3,13] In this study, we optimized a proximity labeling approach in combination with a proteomics-compatible shear stress platform and identified Myo1c as a shear-stress-regulated factor recruited to Jag1 in endothelial cells. In the absence of shear, Myo1c interacts with Jag1, whereas in the presence of shear, this interaction is reduced. Under shear stress, Jag1 polarized downstream of the direction of shear. Knocking down Myo1c inhibited this shear-induced polarization, and pharmacological inhibition of Myo1c reorganized Jag1 in perinuclear structures under static conditions. In addition, upon knockdown of Myo1c, the membrane levels of Jag1 were reduced under static conditions, whereas under shear conditions, this effect trended toward an increase in membrane levels, indicating a complex interplay between Myo1c, shear stress, and Jag1 trafficking. Together, these data reveal

Myo1c as a novel factor responsible for trafficking of Jag1 under hemodynamic loading.

RESULTS

Jag1 polarizes downstream of flow followed by nucleograde transport from the membrane

To study the reorganization of Jag1 under shear, we exposed human umbilical vein endothelial cells (HUVECs) to shear stress in ibidi chamber slides coated with collagen IV and connected to an ibidi pressure pump system. The shear stress was built up linearly in 4 steps over 4 h to 1.8Pa as outlined in STAR Methods. Cells were exposed to shear stress for up to 48 h and either fixed and stained for Jag1 or imaged by live imaging. Shear induced Jag1 reorganization into dynamic substructures downstream of shear. Static condition was used as a control (Figure 1A). In addition to the emergence of reorganized clustering of Jag1 under shear as described before,[14] polarization of Jag1 was observed downstream of the shear direction (Figures 1B and S1A). Early after shear onset, Jag1 rapidly accumulated at the planar pole downstream of shear, followed by nucleograde transport from the membrane (Figures 1C–1E; Videos S1, S2, and S3 [shear] and Videos S4 and S5 [static]). Quantification showed that 64% (SEM = 3.1%) of the cells demonstrated a polarized distribution of Jag1. Live imaging showed that after polarization of Jag1, the endothelial cells migrated in the direction of shear (Videos S1, S2, and S3 and Figure S1B). Under static conditions we rarely observed reorganization of Jag1, only in cases when a cell protrusion retracted (Figure 1A).

Jag1-APEX2 identified shear-sensitive interactors

To identify mechanoresponsive Jag1-interacting factors that contributed to Jag1 trafficking, we took a combined approach of a large surface area shear system and proximity labeling.[14] We genetically attached the engineered ascorbate peroxidase (APEX2) to Jag1. APEX2 labels nearby peptides in the presence of hydrogen peroxide and biotin tyramide (Figure 2A).[15] Tagging the C-terminal intracellular domain of Jag1 enabled labeling of proximal proteins (within a 20 nm radius) in the presence or absence of flow-induced shear stress (Figure 2B). Verification of the construct showed that Lenti-Jag1-APEX2 exhibited a higher molecular weight than endogenous Jag1, as expected (Figure 2C). Of note, shear stress induces cell quiescence leading to reduced number of cells under shear stress conditions as compared to the static condition, as reflected by the decreased actin expression in Figure 2C. For further experiments, cell numbers were controlled to ensure equal cell number and confluency in the different conditions. Localization of the Jag1-APEX2 or APEX2 coupled to nuclear export signal (NES-APEX2) constructs were tested by incubating transduced cells with 500 μM biotin tyramide for 30 min and subsequently adding 1 mM of hydrogen peroxide for 1 min before quenching the reaction. This showed the expected localization of labeling patterns. NES-APEX2 had enriched cytoplasmic labeling, whereas Jag1-APEX2 enriched labeling at the membrane (Figures 2D and 2E). As the shear stress platform, we utilized our previously modeled annular orbital shaker (or dish-in-a-dish) system with more defined and uniform shear characteristics than a simple dish on a shaker (Figures 3A and 3B).[14] To compare static and shear conditions, HUVECs expressing Jag1-APEX2 were cultured statically or exposed to a shear stress between 0.6 and 0.8 Pa for 15 min or 24 h (Figure 3C). Bright-field microscopic images of the cells during the labeling experiment confirmed shear-induced cellular alignment (Figure 3D).[14] The hits from the different shear exposure regimes that were labeled and are candidates for Jag1 proximity are represented in Figure 3E. The genes under each condition were subjected to Gene Ontology (GO) analysis (Figure S2). This analysis revealed proximity of Jag1 to proteins involved in membrane processes, adhesion, and the actomyosin network. Since the Myo1 family of motor proteins is involved in establishing cortical and membrane tension,[16] Myo1c specifically has roles in regulating the presentation of membrane proteins and the stability of cell-cell adhesion,[17,18] and Myo1c recently was shown to augment shear-induced secretion of Von Willebrand Factor (VWF) from Weibel-Palade bodies,[19] we further investigated the Jag1-Myo1c interaction.

Myo1c interacts with and regulates Jag1 localization

Myo1c emerged from the screen as proximal to Jag1 under static conditions but was no longer detected when exposed to shear. To further assess the interaction between Jag1 and Myo1c, we investigated the physical interaction under various conditions and the functional interaction by knockdown or inhibition of Myo1c. Under static conditions, Myo1c co-immunoprecipitated (coIP) with Jag1, whereas under shear (0.8 Pa for 24h), this coIP was reduced (Figures 4A and 4B). We confirmed the interaction between Jag1 and Myo1c in a reverse coIP; however, although there is a trend for reduced interaction under shear, the reduction was not significant (Figures 4C and 4D).

To inhibit Myo1c we used pentachloropseudilin (PCLP), a noncompetitive reversible inhibitor of myosin 1 class proteins, which prevents nucleotide binding by sterically hindering the coupling to the actin-binding site.[20] We first performed coIP experiments in HUVECs treated with 5 μM PCLP for 4 h to assess interference with the interaction between the two proteins. PCLP treatment did not significantly change the interaction between Jag1 and Myo1c (Figures 4E and 4F). PCLP treatment (5 μM) caused perinuclear accumulation of Jag1 in HUVECs within 2 h of exposure. This accumulation increased upon prolonged exposure (Figure 5A). The same effect was also confirmed to occur in cervical cancer HeLa cells for Jag1 (Figures S3A and S3B). These cells were selected for the study as they express Jag1 as well as proteins involved in mechanotransduction, such as the Jag1 interactor vimentin, and have been previously used to test the Myo1c inhibitor PCLP.[21] In the treatment with PCLP, HUVECs were dose sensitive, with lower doses leading to reduced perinuclear accumulation after 16 h (Figure S3C). As effects of PCLP have been reported on the cytoskeleton, which might affect cellular organization, both HeLa cells and HUVECs were stained for actin, microtubules, and intermediate filaments (vimentin), but no changes matching the Jag1 reorganization were visible, although a meshwork like organization of microtubules and vimentin appeared under PCLP treatment (Figure S3D).

After exposure to shear, both Jag1 and Myo1c polarized downstream of flow (visible in the individual fluorescence channels), but the foci traveling toward the nucleus do not colocalize (visible in

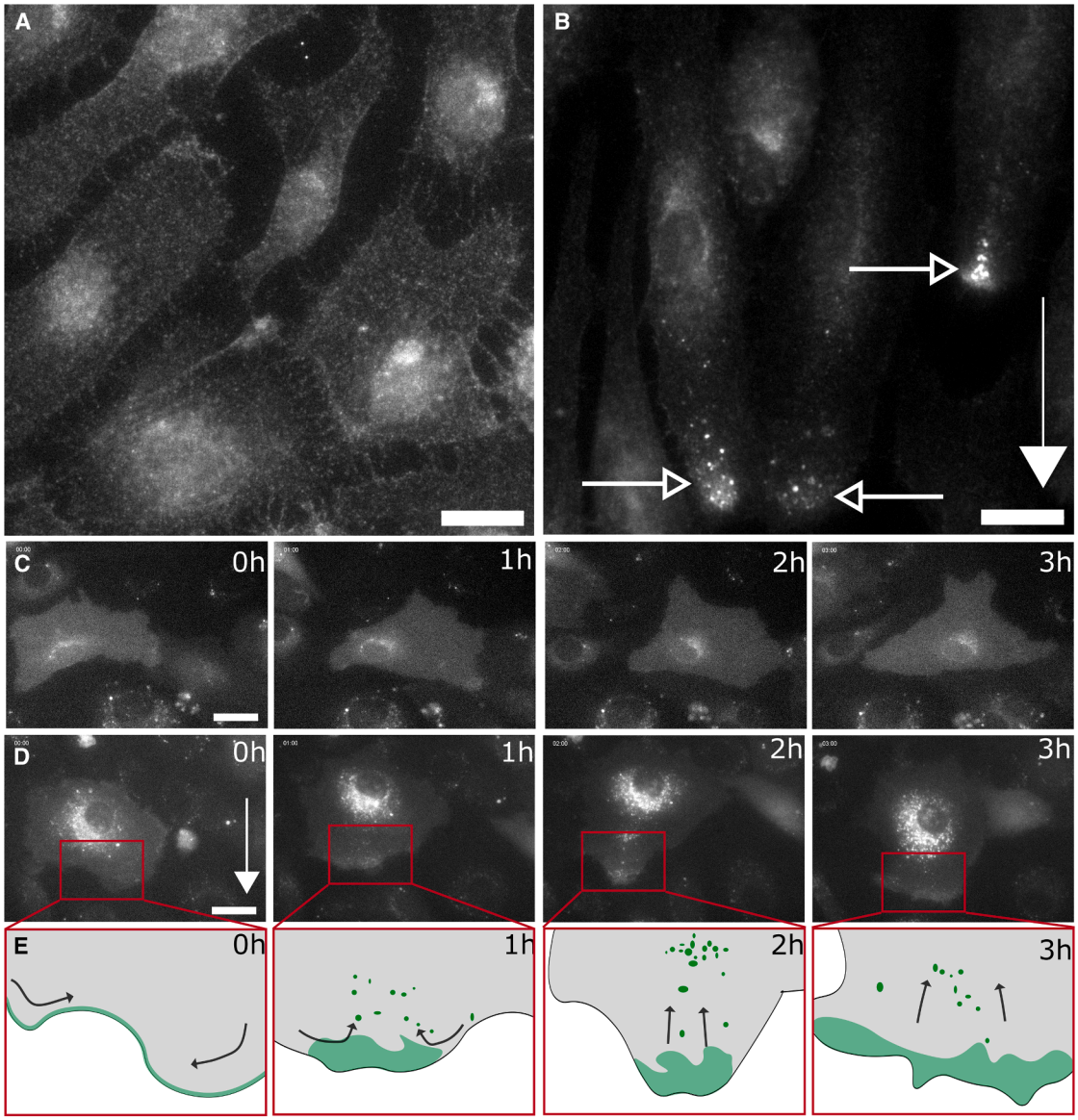

Figure 1. Jagged1 relocalizes in response to shear stress

(A and B) Fluorescence microscopy images of Jag1 immunofluorescence staining. HUVECs were exposed to static (A) and 2-Pa shear stress for 48 h (B) and samples were fixed and stained with a Jag1 antibody. The shear direction is indicated with filled arrows, and shear-induced Jag1 relocalization is indicated with open arrows. 64% (SEM = 3.1%) of cells displayed polarization of Jag1 ($N = 3$, 3 fields of view). Scale bar, 20 μm. See Figure S1A for an expanded field of view of Figure 1B.

(C and D) Stills from live imaging of Jag1eGFP-expressing HUVECs under static (C) or shear (D) conditions. Scale bar, 25 μm. See Videos S1, S2, S3, S4, and S5 for recordings at 4-min intervals.

(E) Manual traces of the cell outline (gray) and shear-induced Jag1 localization (green) observed in the magnification windows (red). Black arrows indicate the direction the Jag1 densities appear to follow. See Figure S1B or Video S1 for additional frames supporting the densities represented here.

the merge) (Figure 5B). Subsequently, we aimed to knockdown Myo1c to verify an effect on Jag1 reorganization. Myo1c could effectively be knocked down in HUVECs, and protein levels were influenced neither by shear application nor by knockdown of other hits identified in the screen (Figures 5C and 5D). Knocking down Myo1c using small interfering RNA and exposing HUVECs to shear revealed that the flow-induced polarization was lost (Figures 5E and S4). Biotinylation of membrane proteins followed by streptavidin pull-down revealed that Jag1 membrane levels were reduced under shear. Knocking down Myo1c significantly reduced Jag1 membrane levels under static conditions. This reduction was not observed under shear; on the contrary, in the Myo1c knockdown, shear induced a trend for an increase of Jag1 membrane levels (Figures 5F and 5G). The proposed Jag1 membrane localization and presentation under static conditions and the shear-induced polarization are presented in Figure 5H.

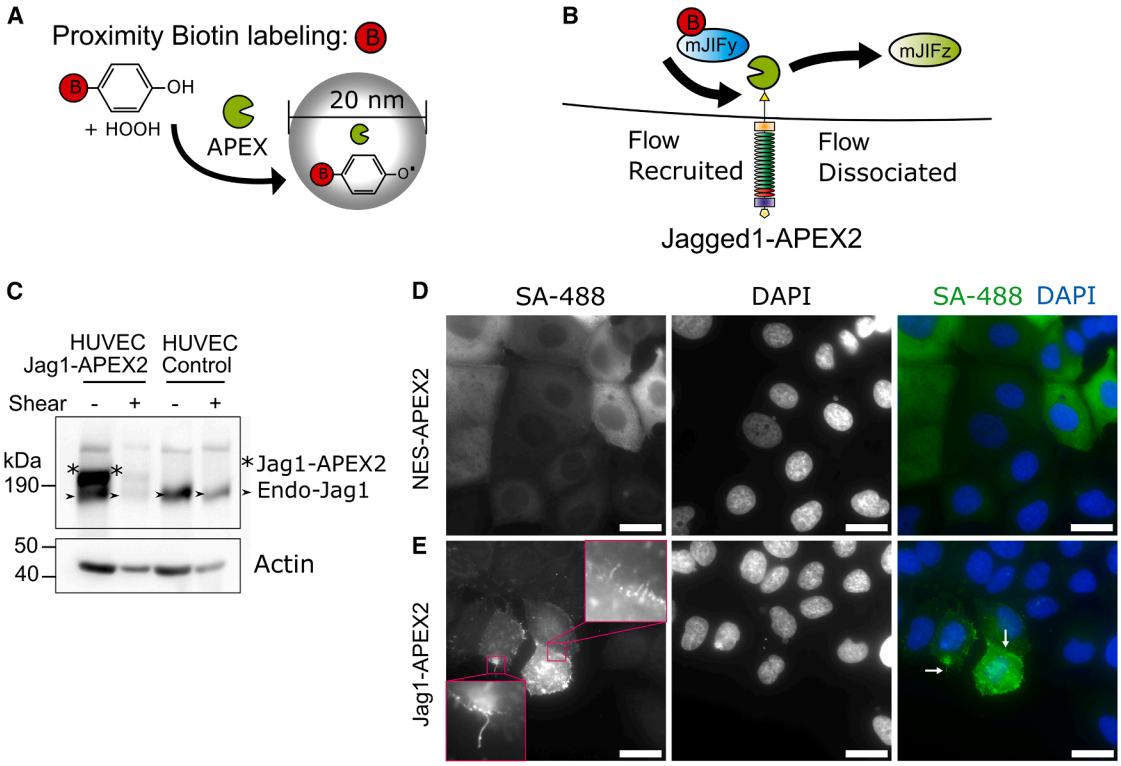

Figure 2. Proximity biotin labeling, mass spectroscopy, and shear platform to identify shear stress-sensitive Jag1-interacting proteins

(A) The engineered ascorbate peroxidase (APEX2) converts biotin tyramide to a free radical-carrying species in the presence H_2O_2, allowing labeling of nearby peptides. Coupling APEX2 to Jag1 and performing labeling interaction under different mechanical loading conditions allows the identification of mechanoresponsive Jagged-interacting factors (mJIFy and mJIFz).

(B) Jag1 engineered with APEX2 on the C-terminal (intracellular) domain enables labeling of cytoplasmic proximal proteins in the presence or absence of flow-induced shear stress.

(C) Immunoblot of Jag1 and Lenti Jag1-APEX2 expressions. HUVECs were transduced with Lenti-Jag1-APEX2, exposed to static or shear conditions, and blotted for Jag1 and Actin.

(D and E) Immunofluorescence microscopy of cells labeled with streptavidin 488 (SA488, green) and 4',6-diamidino-2-phylindole (DAPI; blue). MCF7 cells were transduced with (D) Lenti-APEX2-NES or (E) Lenti-Jag1-APEX2, biotinylated, and stained with streptavidin 488 and DAPI; scale bars, 25 μm.

DISCUSSION

Our study reveals a novel role for Myo1c as a Jag1-interacting shear-responsive motor protein. Myo1c, a member of the myosin 1 family, plays crucial roles in membrane tension and various cellular functions, including nuclear myosin activity and adaptation in vestibular cells.[22–24] In endothelial cells, Myo1c is vital for the membrane presentation of vascular endothelial growth factor receptor 2 (VEGFR2), G-actin transport, integrin trafficking,[17,25] and secretion of VWF.[19] Myo1c regulates protein delivery to and uptake from the plasma membrane under specific signaling cues, as is the case for GLUT4 glucose transporter under insulin signaling in brown fat[26] and E-cadherin uptake and dynamics in epithelial cells.[18] Our data suggest that Myo1c regulates bidirectional Jag1 trafficking and likely plays a role in Jag1 delivery to the plasma membrane under both static and shear conditions, and in Jag1 endocytosis and relocalization under shear (Figure 5).[13] Only a few cytoplasmic tail interactors of Jag1 are currently known. A recent study on the nuclear Jag1 intracellular domain identified several candidate interactors in our screen, including PDIA4 and ANXA2.[27] Other interactors include Mindbomb and Neuralized, both RING ubiquitinases that promote the binding of Epsin and facilitate Jag1 endocytosis and Notch transactivation.[28,29] We previously identified vimentin as a Jag1 interactor and demonstrated that depletion of vimentin increased membrane levels of Jag1 but decreased turnover and signaling.[8,30]

Mutations in the JAG1 gene are a cause of Alagille syndrome, a multiorgan genetic disorder affecting the liver, heart, and eyes. The condition leads to bile duct abnormalities and cholestasis (disrupted bile flow) and characteristic fibrosis.[31] Many JAG1 mutations affect trafficking of Jag1 to the membrane, but how trafficking of endogenous Jag1 ligands is regulated is unknown. Here, we show that Myo1c regulates Jag1's response to shear stress in endothelial cells, which are important for bile duct development. Myo1c has been shown to play a role in hepatic fibrosis, and although its role in cholestasis is unknown, our data indicate that disrupted Myo1c may potentially contribute to bile duct abnormalities. While Myo1c has not been directly linked to congenital heart defects, its role in intracellular

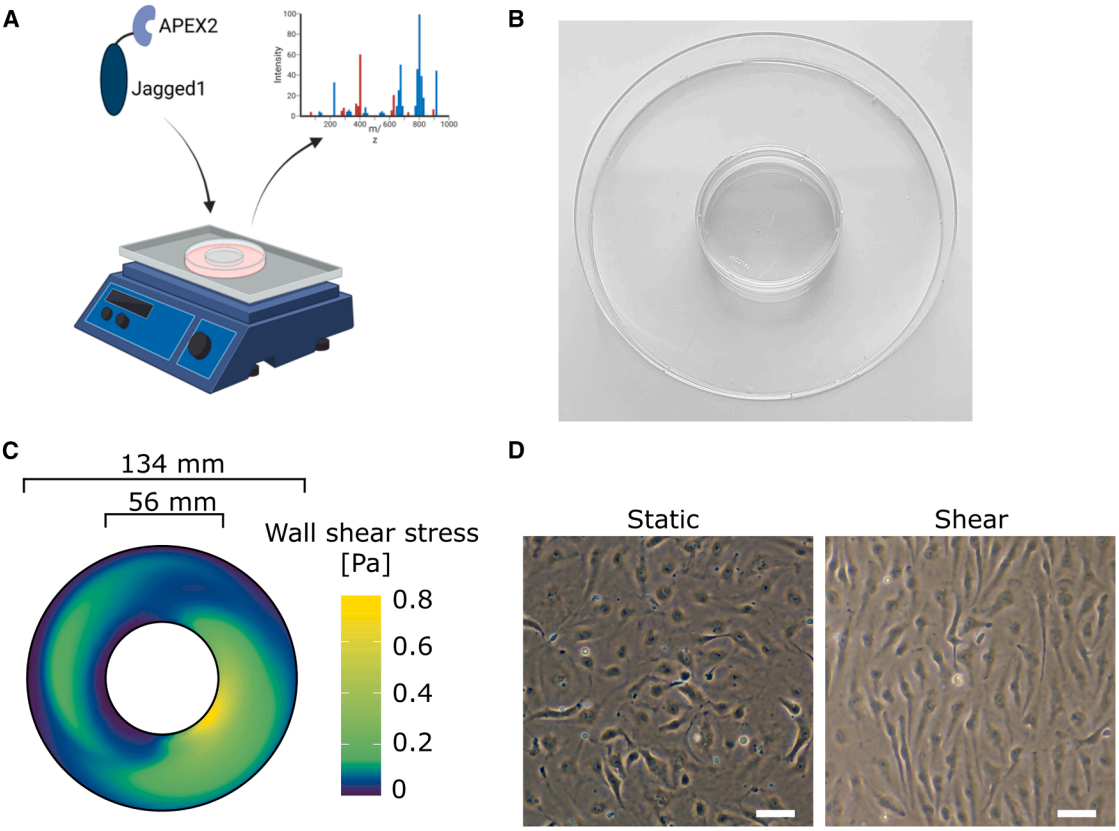

(legend on next page)

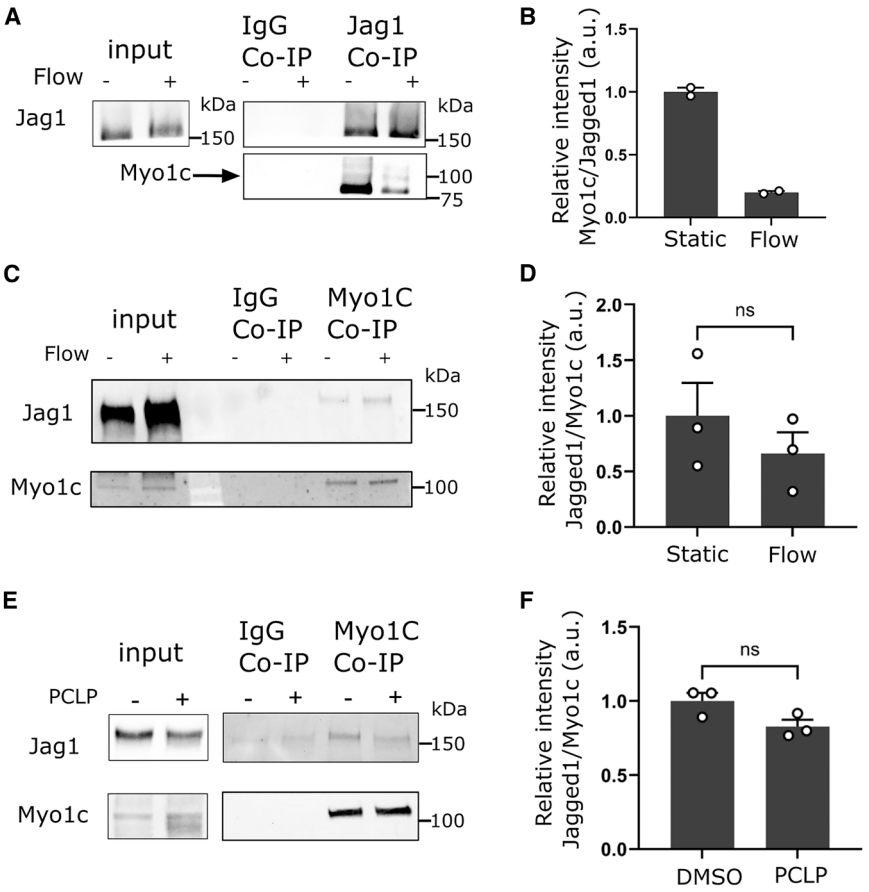

Figure 4. Myo1c differentially interacts with Jag1 under shear stress

(A) Jag1 and Myo1c co-immunoprecipitation. HUVECs cultured under shear (0.8 Pa for 24 h) and static conditions were lysed and immunoprecipitated using an anti-Jag1 antibody. The precipitate was immunoblotted for Myo1c.

(B) Quantification of (A) ($N = 2$).

(C) Myo1c and Jag1 co-immunoprecipitation, reverse pull-down of (A). HUVECs cultured under shear (0.8 Pa for 24 h) and static conditions were lysed and immunoprecipitated using an anti-Myo1c antibody. The precipitate was immunoblotted for Jag1.

(D) Quantification of (C).

(E) Immunoblot analysis of Myo1 co-immunoprecipitated together with Jag1 from HUVECs treated with PCLP. PCLP treatment did not significantly affect Jag1-Myo1c interaction.

(F) Quantification of (E). All experiments were performed three times unless indicated otherwise. The levels are presented as the mean of each replicate relative to their corresponding control +SEM. For western blots HSC-70 were used as a loading control. p values were obtained with GraphPad Prism as described in the methodology. Significance is indicated as ns, $p > 0.05$.

trafficking such as its role in Jagged1 trafficking described here could indirectly affect cardiac morphogenesis.

The mechanisms by which Myo1c alters Jag1 organization and its effects on signaling under shear stress require further exploration. Myo1c facilitates signal-dependent membrane protein presentation, such as VEGF-A-induced VEGFR2 presentation.[17] Its absence reduces VEGFR2 on the plasma membrane, underscoring its role in angiogenesis regulation through modulation of VEGFR2.[17] Jag1 also regulates angiogenesis,[8,32] suggesting additional roles of Myo1c in angiogenesis. Our screen also identified PECAM1 as a potential Jag1 interactor, forming a mechanotransduction complex with VEGFR2.[33] Further investigations on the role of Jagged in this context, especially its polarization under shear stress, are essential. Recent findings indicate that polarized mechanosensitive signaling domains can protect arterial cells from inflammation,[34] suggesting that Jag1 reorganization and its sensitivity to oscillatory shear in aortic cells may play a role in inflammatory signaling in the endothelium.[3]

Limitations of the study

Our study has certain limitations. The influence of sex on the result of the study has not been systematically assessed, and although the HUVECs are from a pooled donor set, it is not clear if sex is a factor in the response of the cells. The APEX2 tag used to identify targets binding to Jag1 was attached to the Jag1 protein through a linker to the C-terminal domain, where a PDZ ligand is located. Possibly, this prevented factors that bind through the PDZ domain from interacting with Jag1. Another possible mechanism of mechanosensitivity was recently also highlighted by the discovery of mechanosensitivity of the Afadin PDZ domain.[35] Afadin is one of the interactors of Jag1 through its PDZ-binding domain.[36] In our screen, the weak and transient Afadin interaction, if relevant in endothelial cells, could not be

Figure 3. Biotin proximity labeling combined with mass spectrometry analyses reveals mechanosensitive Jag1-interacting proteins

(A) Schematic illustration of the fluidic setup to shear endothelial cells, created with Biorender.

(B) Photograph of the shear setup made by gluing a 56-mm dish inside a 134-mm dish.

(C) Visualization of the computational model of the shear stress calculated for the annular culture platform (134 mm outer diameter, 56 mm inner diameter).

(D) Bright-field microscopy images of cells cultured statically (left) or under orbital shaker-induced shear (right); scale bars, 50 μm.

(E) Venn diagram with names of identified proteins. Represented are Jag1-interacting factors that returned a detection event in mass spectrometry screens of three different conditions: static ($N = 2$), 15-min shear ($N = 1$), and 24-h shear ($N = 2$). Only proteins identified in all mass spectrometric screens are denoted in the figure.

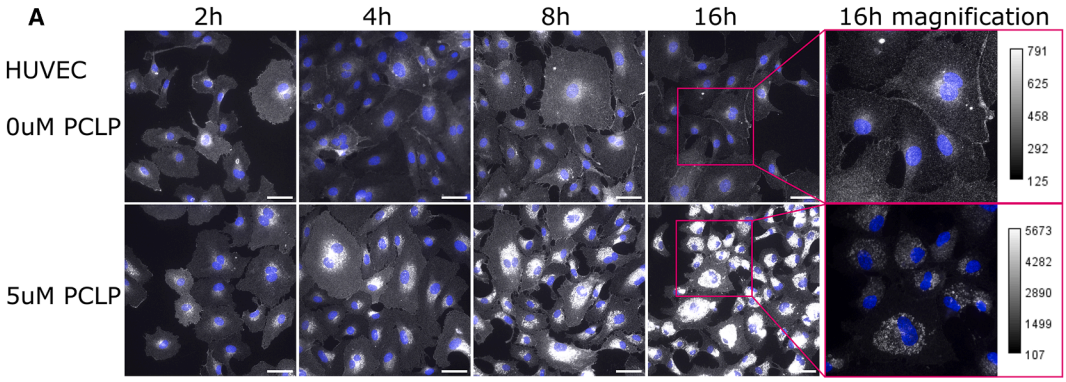

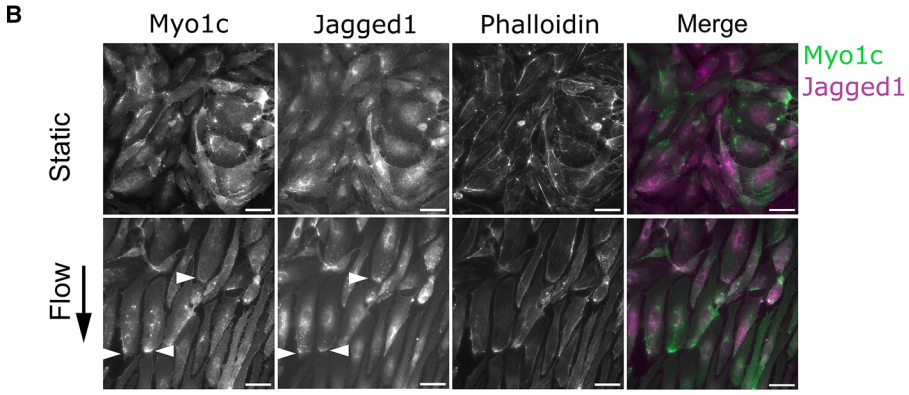

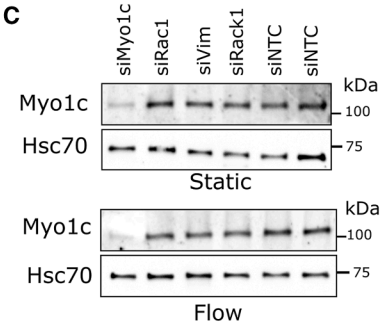

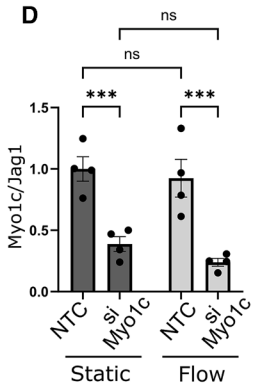

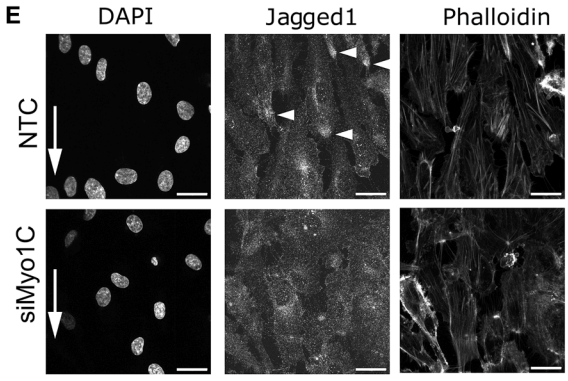

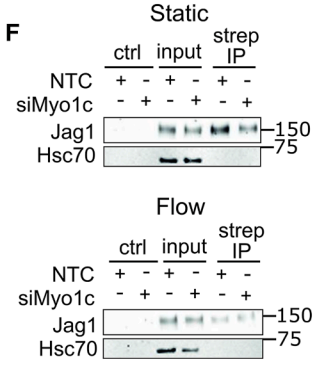

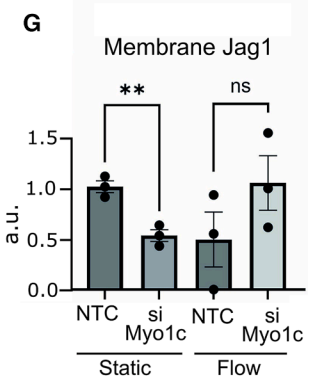

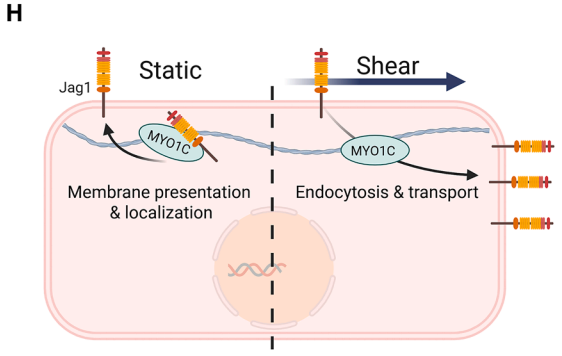

(legend on next page)

detected. In addition, while we functionally and physically confirmed the interaction between Jag1 and Myo1c, although there was a trend in reduction under shear, it was not significant. Alternative protein-protein interaction methods such as proximity ligation assay may shed light on the mechanistic behavior. Notably, while endothelial cells are generally described to migrate against the direction of shear, our observations of migration along the shear direction could arise from experimental conditions, such as growth factor concentrations and shear magnitude.[37,38] Determining how sensitive the regulation is to dynamic changes in shear will be an important future pursuit.

RESOURCE AVAILABILITY

Lead contact

Further information and requests for resources and reagents should be directed to and will be fulfilled by the lead contact Cecilia Sahlgren (cecilia.sahlgren@abo.fi).

Materials availability

Materials are made available upon request.

Data and code availability

- Data: The underlying data have been deposited at the 4TU data repository: https://doi.org/10.4121/d7111159-ca2c-430c-8c29-10ba2a6ca8d7. The proteomics data have also been made available as MassIVE: MSV000099488.
- Code: There is no code associated with this study.
- Other items: There are no other items associated with this study.

STAR★METHODS

Detailed methods are provided in the online version of this paper and include the following:

ACKNOWLEDGMENTS

This project has received funding from the European Research Council (ERC) under grant agreement number 771168 (ForceMorph) and the Academy of Finland under decision numbers 307133, 316882 (SPACE), 330411 (SignalSheets), and 336355 (strategic research profiling area Solutions for Health at Åbo Akademi University). The research has also been supported by the InFLAMES Flagship Programme of the Academy of Finland (decision numbers 337531, 357911, and 359346) and the Åbo Akademi University Foundation's Center of Excellence in Cellular Mechanostasis (CellMech). K.L.L. was supported by the European Union's Horizon 2020 research and innovation program under grant agreement 953234 (Tumor-LN-oC). F.S.R. was supported by The Swedish Cultural Foundation in Finland, Instrumentarium Science Foundation, and Magnus Ehrnrooth Foundation. We would like to extend our gratitude to Tim Wezeman for preparing plasmids during COVID-19 restricted lab access, as well as to Iida Laiho, Jaakko Ahlberg, Meike Hulleman, and Anouk van der Net for help screening initial candidate interactors. We thank Peter Paul Franssen for producing a batch of biotinyl tyramide. We thank the Turku Bioscience Center for discussion of proteomics analysis and for imaging at the Cell Imaging and Cytometry Core. Figure 5H and the graphical abstract were created in BioRender, Sahlgren, C. (2025) https://BioRender.com/vuvo5ek & https://BioRender.com/wytwpzw. pLenti PGK Puro DEST (w529-2) and pENTR1A-GFP-N2 (FR1) were gifts from Eric Campeau and Paul Kaufman (RRID:Addgene_19068 & RRID:Addgene_19364) – cDNA3 APEX2NES was a gift from Alice Ting (RRID:Addgene_49386)).

AUTHOR CONTRIBUTIONS

Conceptualization, O.M.J.A.S. and C.M.S.; methodology, O.M.J.A.S.; software, F.Z.; investigation: O.M.J.A.S., N.V., K.-L.L., F.S.R., M.J.M.H., and G.L.C.; formal analysis, O.M.J.A.S., K.L., N.V., F.S.R., and C.M.S.; resources, C.M.S. and C.V.C.B.; data curation, O.M.J.A.S.; writing – original draft, O.M.J.A.S. and C.M.S.; writing – review & editing, O.M.J.A.S., N.V., K.L., F.S.R., M.J.M.H., F.Z., G.C., C.V.C.B., and C.M.S.; visualization, O.M.J.A.S.;

Figure 5. Myo1c regulates Jag1 localization

(A) Fluorescence microscopy images of HUVECs treated with PCLP for 2, 4, 8 or 16 h and stained for DAPI (blue) and Jag1 (white). Figures from 2 h up to 16 h are represented with same lookup table (LUT); magnified images on the right were scaled with LUTs as indicated to illustrate perinuclear Jag1 organization under PCLP treatment. Scale bars, 50 μm.

(B) Fluorescence microscopy images of HUVECs exposed to shear in parallel ibadi plate channels, stained for Myo1c, Jag1, and actin (phalloidin). Flow-induced polarization of Myo1c and Jagged1 indicated by white arrowheads; scale bars, 50 μm.

(C) Immunoblot analysis of Myo1c expression. HUVECs were exposed to static or shear conditions in a swirling well, and lysates were analyzed for Myo1c levels with different Jag1-interacting candidate knockdowns.

(D) Quantification of Myo1c knockdown efficiency by small interfering RNA (siRNA), normalized for static NTC (non-targeting control). The average knockdown efficiency was 68%.

(E) Confocal fluorescence microscopy of HUVECs under shear or static culture. HUVECs were treated with Myo1c siRNA or NTC and stained for Actin and Jag1. Scale bars, 20 μm. Myo1c staining and static conditions corresponding to this experiment displayed in Figure S4. Representative of three independent experiments.

(F) Immunoblot of membrane proteins of HUVECs treated with siMyo1c or NTC, under static conditions and shear (200 rpm, 0.8 Pa) stained for Jag1 and HSC70. ctrl, nonbiotinylated control; Strep IP, streptavidin pull-down.

(G) Quantification of three independent experiments. All experiments were performed three times. The levels are presented as the mean of each replicate relative to their corresponding control + SEM. For WBs, HSC-70 was used as a loading control. p values were obtained with GraphPad Prism as described in STAR Methods. Significance is indicated as ns, $p > 0.05$; $^{**}p < 0.01$, $^{***}p < 0.001$, $^{****}p < 0.0001$.

(H) Schematic representation of possible Myo1c and Jag1 interaction in the presence and absence of shear. Produced with Biorender.

supervision, C.M.S. and C.V.C.B.; project administration, O.M.J.A.S. and C.M.S.; funding acquisition, C.M.S. and C.V.C.B.

DECLARATION OF INTERESTS

The authors declare no competing interests.

SUPPLEMENTAL INFORMATION

Supplemental information can be found online at https://doi.org/10.1016/j.isci.2025.113879.

Received: April 7, 2025
Revised: July 3, 2025
Accepted: October 23, 2025
Published: October 30, 2025

REFERENCES

1. Foot, N., Henshall, T., and Kumar, S. (2017). Ubiquitination and the regulation of membrane proteins. Physiol. Rev. *97*, 253–281. https://doi.org/10.1152/physrev.00012.2016.
2. Masek, J., and Andersson, E.R. (2017). The developmental biology of genetic Notch disorders. Development *144*, 1743–1763. https://doi.org/10.1242/dev.148007.
3. Souilhol, C., Serbanovic-Canic, J., Fragiadaki, M., Chico, T.J., Ridger, V., Roddie, H., and Evans, P.C. (2020). Endothelial responses to shear stress in atherosclerosis: a novel role for developmental genes. Nat. Rev. Cardiol. *17*, 52–63. https://doi.org/10.1038/s41569-019-0239-5.
4. Souilhol, C., Ayllon, B.T., Li, X., Diagbouga, M.R., Zhou, Z., Canham, L., Roddie, H., Pirri, D., Chambers, E.V., Dunning, M.J., et al. (2022). JAG1-NOTCH4 mechanosensing drives atherosclerosis. Sci. Adv. *8*, eabo7958. https://doi.org/10.1126/sciadv.abo7958.
5. Stassen, O.M.J.A., Ristori, T., and Sahlgren, C.M. (2020). Notch in mechanotransduction – from molecular mechanosensitivity to tissue mechanostasis. J. Cell Sci. *133*, jcs250738. https://doi.org/10.1242/jcs.250738.
6. Bray, S.J. (2016). Notch signalling in context. Nat. Rev. Mol. Cell Biol. *17*, 722–735. https://doi.org/10.1038/nrm.2016.94.
7. Antfolk, D., Antila, C., Kemppainen, K., Landor, S.K.J., and Sahlgren, C. (2019). Decoding the PTM-switchboard of Notch. Biochim. Biophys. Acta. Mol. Cell Res. *1866*, 118507. https://doi.org/10.1016/j.bbamcr.2019.07.002.
8. Antfolk, D., Sjöqvist, M., Cheng, F., Isoniemi, K., Duran, C.L., Rivero-Muller, A., Antila, C., Niemi, R., Landor, S., Bouten, C.V.C., et al. (2017). Selective regulation of Notch ligands during angiogenesis is mediated by vimentin. Proc. Natl. Acad. Sci. USA *114*, E4574–E4581. https://doi.org/10.1073/pnas.1703057114.
9. Seib, E., and Klein, T. (2021). The role of ligand endocytosis in notch signalling. Biol. Cell *113*, 401–418. https://doi.org/10.1111/boc.202100009.
10. Sunshine, H.L., Cicchetto, A.C., Kaczor-Urbanowicz, K.E., Ma, F., Pi, D., Symons, C., Turner, M., Shukla, V., Christofk, H.R., Vallim, T.A., et al. (2024). Endothelial Jagged1 levels and distribution are post-transcriptionally controlled by ZFP36 decay proteins. Cell Rep. *43*, 113627. https://doi.org/10.1016/j.celrep.2023.113627.
11. Suarez Rodriguez, F., Sanlidag, S., and Sahlgren, C. (2023). Mechanical regulation of the Notch signaling pathway. Curr. Opin. Cell Biol. *85*, 102244. https://doi.org/10.1016/j.ceb.2023.102244.
12. Luca, V.C., Kim, B.C., Ge, C., Kakuda, S., Wu, D., Roein-Peikar, M., Haltiwanger, R.S., Zhu, C., Ha, T., and Garcia, K.C. (2017). Notch-Jagged complex structure implicates a catch bond in tuning ligand sensitivity. Science *355*, 1320–1324. https://doi.org/10.1126/science.aaf9739.
13. Driessen, R.C.H., Stassen, O.M.J.A., Sjöqvist, M., Suarez Rodriguez, F., Grolleman, J., Bouten, C.V.C., and Sahlgren, C.M. (2018). Shear stress induces expression, intracellular reorganization and enhanced Notch activation potential of Jagged1. Integr. Biol. *10*, 719–726. https://doi.org/10.1039/c8ib00036k.
14. Driessen, R., Zhao, F., Hofmann, S., Bouten, C., Sahlgren, C., and Stassen, O. (2020). Computational characterization of the dish-in-a-dish, a high yield culture platform for endothelial shear stress studies on the orbital shaker. Micromachines *11*, 552. https://doi.org/10.3390/MI11060552.
15. Hung, V., Lam, S.S., Udeshi, N.D., Svinkina, T., Guzman, G., Mootha, V.K., Carr, S.A., and Ting, A.Y. (2017). Proteomic mapping of cytosol-facing outer mitochondrial and ER membranes in living human cells by proximity biotinylation. eLife *6*, e24463. https://doi.org/10.7554/eLife.24463.
16. McIntosh, B.B., and Ostap, E.M. (2016). Myosin-I molecular motors at a glance. J. Cell Sci. *129*, 2689–2695. https://doi.org/10.1242/jcs.186403.
17. Tiwari, A., Jung, J.J., Inamdar, S.M., Nihalani, D., and Choudhury, A. (2013). The myosin motor Myo1c is required for VEGFR2 delivery to the cell surface and for angiogenic signaling. Am. J. Physiol. Heart Circ. Physiol. *304*, H687–H696. https://doi.org/10.1152/ajpheart.00744.2012.
18. Tokuo, H., and Coluccio, L.M. (2013). Myosin-1c regulates the dynamic stability of E-cadherin-based cell-cell contacts in polarized Madin-Darby canine kidney cells. Mol. Biol. Cell *24*, 2820–2833. https://doi.org/10.1091/mbc.E12-12-0884.
19. El-Mansi, S., Mitchell, T.P., Mobayen, G., McKinnon, T.A.J., Miklavc, P., Frick, M., and Nightingale, T.D. (2024). Myosin-1C augments endothelial secretion of von Willebrand factor by linking contractile actomyosin machinery to the plasma membrane. Blood Adv. *8*, 4714–4726. https://doi.org/10.1182/bloodadvances.2024012590.
20. Chinthalapudi, K., Taft, M.H., Martin, R., Heissler, S.M., Preller, M., Hartmann, F.K., Brandstaetter, H., Kendrick-Jones, J., Tsiavaliaris, G., Gutzeit, H.O., et al. (2011). Mechanism and specificity of pentachloropseudilin-mediated inhibition of myosin motor activity. J. Biol. Chem. *286*, 29700–29708. https://doi.org/10.1074/jbc.M111.239210.
21. Brandstaetter, H., Kishi-Itakura, C., Tumbarello, D.A., Manstein, D.J., and Buss, F. (2014). Loss of functional MYO1C/myosin 1c, a motor protein involved in lipid raft trafficking, disrupts autophagosome-lysosome fusion. Autophagy *10*, 2310–2323. https://doi.org/10.4161/15548627.2014.984272.
22. Batters, C., Arthur, C.P., Lin, A., Porter, J., Geeves, M.A., Milligan, R.A., Molloy, J.E., and Coluccio, L.M. (2004). Myo1c is designed for the adaptation response in the inner ear. EMBO J. *23*, 1433–1440. https://doi.org/10.1038/sj.emboj.7600169.
23. Gillespie, P.G. (2004). Myosin I and adaptation of mechanical transduction by the inner ear. Philos. Trans. R. Soc. Lond. B Biol. Sci. *359*, 1945–1951. https://doi.org/10.1098/rstb.2004.1564.
24. Venit, T., Semesta, K., Farrukh, S., Endara-Coll, M., Havalda, R., Hozak, P., and Percipalle, P. (2020). Nuclear myosin 1 activates p21 gene transcription in response to DNA damage through a chromatin-based mechanism. Commun. Biol. *3*, 115. https://doi.org/10.1038/s42003-020-0836-1.
25. Cota Teixeira, S., Silva Lopes, D., Santos da Silva, M., Cordero da Luz, F.A., Cirilo Gimenes, S.N., Borges, B.C., Alves da Silva, A., Alves Martins, F., Alves Dos Santos, M., Teixeira, T.L., et al. (2019). Pentachloropseudilin Impairs Angiogenesis by Disrupting the Actin Cytoskeleton, Integrin Trafficking and the Cell Cycle. Chembiochem *20*, 2390–2401. https://doi.org/10.1002/cbic.201900203.
26. Boguslavsky, S., Chiu, T., Foley, K.P., Osorio-Fuentealba, C., Antonescu, C.N., Bayer, K.U., Bilan, P.J., and Klip, A. (2012). Myo1c binding to submembrane actin mediates insulin-induced tethering of GLUT4 vesicles. Mol. Biol. Cell *23*, 4065–4078. https://doi.org/10.1091/mbc.E12-04-0263.
27. Kim, E.J., Kim, J.Y., Kim, S.O., Hong, N., Choi, S.H., Park, M.G., Jang, J., Ham, S.W., Seo, S., Lee, S.Y., et al. (2022). The oncogenic JAG1 intracellular domain is a transcriptional cofactor that acts in concert with DDX17/SMAD3/TGIF2. Cell Rep. *41*, 111626. https://doi.org/10.1016/j.celrep.2022.111626.

28. Langridge, P.D., and Struhl, G. (2017). Epsin-Dependent Ligand Endocytosis Activates Notch by Force. Cell *171*, 1383–1396.e12. https://doi.org/10.1016/j.cell.2017.10.048.

29. Lee, H.J., Yoon, J.H., Ahn, J.S., Jo, E.H., Kim, M.Y., Lee, Y.C., Kim, J.W., Ann, E.J., and Park, H.S. (2015). Fe65 negatively regulates Jagged1 signaling by decreasing Jagged1 protein stability through the E3 ligase Neuralized-like 1. Biochim. Biophys. Acta *1853*, 2918–2928. https://doi.org/10.1016/j.bbamcr.2015.08.009.

30. van Engeland, N.C.A., Suarez Rodriguez, F., Rivero-Müller, A., Ristori, T., Duran, C.L., Stassen, O.M.J.A., Antfolk, D., Driessen, R.C.H., Ruohonen, S., Ruohonen, S.T., et al. (2019). Vimentin regulates Notch signaling strength and arterial remodeling in response to hemodynamic stress. Sci. Rep. *9*, 12415. https://doi.org/10.1038/s41598-019-48218-w.

31. Mašek, J., and Andersson, E.R. (2024). Jagged-mediated development and disease: Mechanistic insights and therapeutic implications for Alagille syndrome. Curr. Opin. Cell Biol. *86*, 102302. https://doi.org/10.1016/j.ceb.2023.102302.

32. Benedito, R., Roca, C., Sörensen, I., Adams, S., Gossler, A., Fruttiger, M., and Adams, R.H. (2009). The Notch Ligands Dll4 and Jagged1 Have Opposing Effects on Angiogenesis. Cell *137*, 1124–1135. https://doi.org/10.1016/j.cell.2009.03.025.

33. Coon, B.G., Baeyens, N., Han, J., Budatha, M., Ross, T.D., Fang, J.S., Yun, S., Thomas, J.L., and Schwartz, M.A. (2015). Intramembrane binding of VE-cadherin to VEGFR2 and VEGFR3 assembles the endothelial mechanosensory complex. J. Cell Biol. *208*, 975–986. https://doi.org/10.1083/jcb.201408103.

34. Hong, S.G., Ashby, J.W./, Kennelly, J.P., Wu, M., Steel, M., Chattopadhyay, E., Foreman, R., Tontonoz, P., Tarling, E.J., Turowski, P., et al. (2024). Mechanosensitive membrane domains regulate calcium entry in arterial endothelial cells to protect against inflammation. J. Clin. Investig. *134*, e175057. https://doi.org/10.1172/JCI175057.

35. Vachharajani, V.T., DeJong, M.P., and Dunn, A.R. (2023). PDZ Domains from the Junctional Proteins Afadin and ZO-1 Act as MechanosensorsPreprint. bioRxiv. https://doi.org/10.1101/2023.09.24.559210.

36. Hock, B., Böhme, B., Karn, T., Yamamoto, T., Kaibuchi, K., Holtrich, U., Holland, S., Pawson, T., Rübsamen-Waigmann, H., and Strebhardt, K. (1998). PDZ-domain-mediated interaction of the Eph-related receptor tyrosine kinase EphB3 and the ras-binding protein AF6 depends on the kinase activity of the receptor. Proc. Natl. Acad. Sci. USA *95*, 9779–9784. https://doi.org/10.1073/pnas.95.17.9779.

37. Park, H., Furtado, J., and Poulet, M. (2021). Defective Flow-Migration Coupling Causes Arteriovenous Malformations in Hereditary Hemorrhagic Telangiectasia. Circulation *144*, 805–822. https://doi.org/10.1161/CIRCULATIONAHA.120.053047.

38. Vion, A.C., Perovic, T., Petit, C., Hollfinger, I., Bartels-Klein, E., Frampton, E., Gordon, E., Claesson-Welsh, L., and Gerhardt, H. (2020). Endothelial Cell Orientation and Polarity Are Controlled by Shear Stress and VEGF Through Distinct Signaling Pathways. Front. Physiol. *11*, 623769. https://doi.org/10.3389/fphys.2020.623769.

39. Lam, S.S., Martell, J.D., Kamer, K.J., Deerinck, T.J., Ellisman, M.H., Mootha, V.K., and Ting, A.Y. (2015). Directed evolution of APEX2 for electron microscopy and proximity labeling. Nat. Methods *12*, 51–54. https://doi.org/10.1038/nmeth.3179.

40. Campeau, E., Ruhl, V.E., Rodier, F., Smith, C.L., Rahmberg, B.L., Fuss, J.O., Campisi, J., Yaswen, P., Cooper, P.K., and Kaufman, P.D. (2009). A versatile viral system for expression and depletion of proteins in mammalian cells. PLoS One *4*, e6529. https://doi.org/10.1371/journal.pone.0006529.

41. Schneider, C.A., Rasband, W.S., and Eliceiri, K.W. (2012). NIH Image to ImageJ: 25 years of image analysis. Nat. Methods *9*, 671–675. https://doi.org/10.1038/nmeth.2089.

42. Reimand, J., Kull, M., Peterson, H., and Hansen, J. (2007). g:Profiler-a web-based toolset for functional profiling of gene lists from large-scale experiments. Nucleic Acids Res. *35*, W193–W200. https://doi.org/10.1093/nar/gkm226.

43. Wenger, C.D., and Coon, J.J. (2013). A proteomics search algorithm specifically designed for high-resolution tandem mass spectra. J. Proteome Res. *12*, 1377–1386. https://doi.org/10.1021/pr301024c.

44. Sakaue-Sawano, A., Kurokawa, H., Morimura, T., Hanyu, A., Hama, H., Osawa, H., Kashiwagi, S., Fukami, K., Miyata, T., Miyoshi, H., et al. (2008). Visualizing Spatiotemporal Dynamics of Multicellular Cell-Cycle Progression. Cell *132*, 487–498. https://doi.org/10.1016/j.cell.2007.12.033.

45. Hung, V., Udeshi, N.D., Lam, S.S., Loh, K.H., Cox, K.J., Pedram, K., Carr, S.A., and Ting, A.Y. (2016). Spatially resolved proteomic mapping in living cells with the engineered peroxidase APEX2. Nat. Protoc. *11*, 456–475. https://doi.org/10.1038/nprot.2016.018.

STAR★METHODS

KEY RESOURCES TABLE

REAGENT or RESOURCE	SOURCE	IDENTIFIER
Antibodies		
Myo1c	Santa Cruz Biotechnology	Cat#sc-136544; RRID:AB_10649358
Jag1	Cell Signaling Technology	Cat#2620; RRID:AB_10693295
Bacterial and virus strains		
NBE Stable *E. coli*	New England Biolabs	Cat# C1010S
Chemicals, peptides, and recombinant proteins		
Pentachloropseudilin	Aobious	Cat#AOB33969
cOmplete Protease Inhibitor Cocktail	Roche	Cat#4693116001
Critical commercial assays		
Miniprep protocols kit	Qiagen	Cat#27106
Midiprep protocols kit	Nucleobond	Cat#740410.50
Deposited data		
Raw and analyzed data	This paper	https://doi.org/10.4121/d7111159-ca2c-430c-8c29-10ba2a6ca8d7
APEX2 biotinylation mass spectrometry	This paper	MSV000099488
Experimental models: Cell lines		
Human Umbilical Vein Endothelial Cells	Lonza	Cat#C2519A
HEK293T	ECACC	Cat# 12022001
MCF7	ATCC	Cat# HTB-22
HeLa	ATCC	Cat# CRM-CCL-2
Oligonucleotides		
ON-TARGETplus siRNA SMARTpool targeting human MYO1C	Dharmacon Reagents	Cat#L-015121-00
ON-TARGETplus control siRNA SMARTpool	Dharmacon Reagents	Cat#D-001810-10
Forward primers for JAG1-APEX2 generation:TATTATCTAGATTATTTGT CATCATCGTCCTTATAATCGGCG and	This paper	–
Reverse primers for JAG1-APEX2 generation: CGAATGGAGTACATCGTAGGGGAT	This paper	–
Recombinant DNA		
pLenti Jag1-APEX2	This paper	–
pcDNA3 APEX2-NES	Lam et al.[39] (Alice Ting)	RRID:Addgene_49386
pLenti pCMVR8.74	Depositing Lab: Didier Trono (Unpublished)	RRID:Addgene_22036
pLenti pMD2.G	Depositing Lab: Didier Trono (Unpublished)	RRID:Addgene_12259
pLenti PGK Puro DEST (w529-2)	Campeau et al.[40] (Eric Campeau & Paul Kaufman)	RRID:Addgene_19068
pENTR1A-GFP-N2 (FR1)	Campeau et al.[40] (Eric Campeau & Paul Kaufman)	RRID:Addgene_19364
pLenti Jag1-eGFP	This paper	–
Software and algorithms		
ImageJ	Schneider et al.[41]	https://imagej.nih.gov/ij/
g:Gost (version e101_e.g.,48_p14_baf17f0)	Reimand et al.[42]	biit.cs.ut.ee/gprofiler/gost

(*Continued on next page*)

Continued

REAGENT or RESOURCE	SOURCE	IDENTIFIER
MetaMorpheus (version 0.0.303)	Wenger et al.[43]	https://smith-chem-wisc.github.io/MetaMorpheus/
Other		
Streptavidin agarose beads	Thermo Scientific	Cat#20353
Pierce A/G magnetic beads	Thermo Scientific	Cat#88803

EXPERIMENTAL MODEL AND STUDY PARTICIPANT DETAILS

Cell culture

Human Umbilical Vein Endothelial Cells (Lonza, pooled, mixed gender, Cat#C2519A) were cultured in Endothelial Cell Basal Media 2 (Promocell, Cat#C-22011) supplemented with Growth Medium 2 supplement mix. This consists of the following supplements and final concentrations: Fetal Calf Serum (0.02 mL/mL), Epidermal Growth Factor (recombinant human) (5 ng/mL), Basic Fibroblast Growth Factor (recombinant human) (10 ng/mL), Insulin-like Growth Factor (Long R3 IGF, recombinant human) (20 ng/mL), Vascular Endothelial Growth Factor 165 (recombinant human) (0.5 ng/mL), Ascorbic Acid (1 μg/mL), Heparin (22.5 μg/mL), Hydrocortisone (0.2 μg/mL). HEK293T (ECACC, female), MCF7 (ATCC, female), and HeLa cells (female) used for producing and testing lentivirus and PCLP assays were cultured in DMEM high glucose (Gibco, Cat#41966) supplemented with 10% fetal bovine serum, 100 units/ml penicillin, and 100 μg/ml streptomycin. All cell cultures were maintained at 37°C and 5% CO2 in a humidified incubator and passaged twice per week.

Plasmids

To introduce Jag1-APEX2 into endothelial cells a pLenti Jag1-APEX2 lentivirus plasmid was constructed. pcDNA3 Jag1-APEX2-mKO2 was synthesized as the open reading frame (ORF) from NM_000214.2 (Baseclear, Leiden, NL), coupled with a GDPPVAT linker to the APEX2 ORF including FLAG tag from the Alice Ting lab,[39] a TRTRPLE linker, and the mKO2 sequence.[44] To target HUVEC, a lentiviral variant without mKO2, due to size restrictions, was made by PCRing JAG1-APEX2 with the primers FW:TATTATCTAGATTATTTGTCATCATCGTCCTTATAATCGGCG and RV:CGAATGGAGTACATCGTAGGGGATCC, and cloned with XbaI and BamhI into pENTR1a (addgene #19364),[40] and subsequently transferred to pLenti-DEST (Addgene #19068)[40] using gateway recombination (LR-clonase 2). As control plasmid for the proximity labeling we used an APEX2 domain coupled to a nuclear export signal (NES) for cytoplasmic labeling. pcDNA3 APEX2-NES (RRID:Addgene_49386) was a gift from Alice Ting through Addgene.

The transfer plasmid for live imaging Jag1, pLenti Jag1-eGFP, was created through replacing the APEX2 in pENTR-Jag1-APEX2 with eGFP and recombination through the gateway method. Plasmids were expanded in NEB Stable and isolated using standard miniprep protocols (Qiagen), or midiprep protocols (Nucleobond).

Lentiviral production and transduction

Lentivirus was produced by transfecting pLenti transfer plasmid, pCMVR8.74, and pMD2.G into HEK293T cells using PEI transfection. Medium was harvested in the 3 days following transfection, precleared by 500 g centrifugation and filtered through a 0.45 μm syringe filter. Filtered medium was centrifuged for 120 min at 50,000 g at 16°C and pellets were resuspended in 1x PBS for storage at 80°C and transduction. pCMVR8.74 and pMD2.G were a gift from Didier Trono (RRID:Addgene_22036 and RRID:Addgene_12259).

METHOD DETAILS

Mechanoresponsive Jagged interacting factor identification

Labeling and isolation of interacting factors through APEX2 were performed as described before.[45] HUVECs were transduced with Lenti Jag1-APEX2, cultured at 17,000 cells/cm2 on Collagen IV coated annular culture vessels (Dish-in-a-Dish) of 13.5 cm outer diameter and 5.6 cm inner diameter.[14] Confluent cells were cultured under static (n = 2) or shear conditions (15 min (n = 1) or 24 h (n = 2), 150 rpm, 3 mm medium height, 1 cm orbit diameter, resulting in a shear between 0.6 and 0.8 Pa (6–8 dyne/cm^2), and subsequently cultured for 30 min under static or shear conditions in the presence of 500 μM biotin-tyramide. Biotin labeling was initiated by adding 0.1% hydrogen peroxide for 60 s after which the reaction was quenched by washing 3× with PBS supplemented with quencher (5 mM trolox, 10 mM sodium ascorbate and 10 mM sodium azide). Samples were then lysed in RIPA (50 mM Tris, 150 mM NaCl, 0.1% w/v SDS, 0.5% w/v sodium deoxycholate, 1% Triton) supplemented with Complete protease inhibitor (PI; Roche) and quencher (RIPAPIQ). To isolate biotinylated proteins, magnetic streptavidin beads (Pierce) were equilibrated in RIPAPIQ. The samples were incubated with the beads under constant agitation for at least 4 h or overnight at 4°C. Beads were washed two times with RIPA, subsequently with 1M KCl, then 0.1M Na2CO3, then 2M Urea in 10 mM TrisHCl, and twice with

RIPA again. Reduction and alkylation occurred by incubation with 10 mM DTT in 100 mM Ammonium Bicarbonate and 100 μl of 55 mM iodoacetamide for 1 h each, and a final incubation in 10 mM DTT, 8 mM iodoacetamide in 100 mM ammonium bicarbonate. Finally, bead-bound products were cleaved with 1 μg mass spectrometry grade trypsin. Cleaved product was freeze-dried and analyzed by mass spectrometry on a TripleTOF5600 (Sciex). Sample Spectra were analyzed using MetaMorpheus version 0.0.303 to identify peptide spectrum matches.[43]

Total membrane protein biotinylation

HUVECs exposed to static or shear conditions for 24 h were placed on ice and washed three times with ice-cold PBS-CM (0.5 mM MgCl2 and 0.9 mM CaCl2), followed by membrane protein labeling with 0.5 mg/mL EZlink sulfo-NHS-SS-biotin (Thermo Scientific, 21331) in PBS for 30 min on ice. Afterward, the cells were washed twice with ice-cold 0.1 M glycine in PBS, then twice with PBS-CM. The cells were lysed in RIPA+PI (RIPA buffer with cOmplete Protease Inhibitor Cocktail (Roche, 4693116001)) for 10 min on ice and centrifuged at 15,000 rpm for 10 min at 4°C. The supernatant was incubated in streptavidin agarose beads (Thermo Scientific, 20353) and incubated overnight at 4°C with a rotary shaker. The next day, samples were centrifuged at 14,000 rpm for 30 s and washed with RIPA+PI three times. The pellet was resuspended in Laemmli sample buffer for western blot.

Coimmunoprecipitation

Cells were lysed with lysis buffer (50 mM Tris (pH 7.5), 150 mM NaCl, 1% Triton X-100, 0.1% SDS, supplemented with protease and phosphatase inhibitors). Samples were cleared using a Branson sonifier three times for 5 s and spun down at 14k g. Beads were washed before use, three times with 50 mM Tris-HCl (pH 7.5); 250 mM NaCl; 0.1% NP-40. Samples were pre-cleared and allowed to conjugate to antibody overnight. Proteins were coIPed with Pierce Protein A/G magnetic beads (Thermo Scientific, 88803) and western blot was performed. Laemmli was used as a sample buffer and loading was measured using Revert 700 Total Protein Stain (LICOR).

Western blotting

Cells were washed with 4°C PBS and incubated with RIPA lysis buffer at 4°C for 20 min after which the contents of the wells were harvested. Samples were centrifuged at ≥10,000 g, at 4°C and the supernatant was retained. 4x Laemmli buffer was added to the supernatant and heated for 5 min at 95°C. SDS-Page (sodium dodecyl sulfate polyacrylamide gel electrophoresis) with precast gels (12% or 4–12% gradient gels; Biorad) were used to separate proteins. Proteins were transferred to a nitrocellulose membrane (Amersham, Protran). Both the separation and the transfer of the proteins was carried out in a wet transfer blotting system (Biorad) at 100 V. Membranes were blocked with 5% nonfat dry milk in PBS with 0.1% Tween, for 1h at room temperature. Primary staining on the membranes was performed overnight at 4°C. The membranes were then washed 3x in PBS 0.1% Tween and a secondary staining with HRP-coupled antibodies was done for 1h at room temperature. The membranes were washed at least 3x after secondary staining. Detection was performed with a ECL chemiluminescence kit on an iBright CL1500 (Invitrogen).

Shear stress live imaging

HUVECs transduced with Lenti Jag1-eGFP were sheared in a parallel plate setup (ibidi). This was placed on a Leica DMI8 microscope, with a Leica EL6000 as light source, an HC PL APO 40x/0.95 air objective, and a filter set of 450–490/500/500–550 for imaging eGFP. Cells were cultured at a density of 50,000 cells/cm^2 in μ-slides VI 0.4, coated with collagen IV (ibidi, cat.# 80602) and connected to an ibidi pressure pump system in the incubation box of the microscope. At the start of an imaging experiment shear stress was built up linearly in 4 steps over 4 h to the final desired shear stress of 1.8 Pa (18 dyne/cm^2). Images were acquired with a Hamamatsu-C13440-20CU-US-300708 camera, every 4 min, with a 2s exposure for the Jag1-eGFP channel. Live recordings were processed to remove bright outlier (hot) pixels, by ''remove outliers'' in ImageJ (radius 2.0, threshold 100).

Immunocytochemistry

Cells after static and shear treatment were fixed with 4% PFA for 10 min at room temperature, followed by permeabilization at room temperature with 0.1% Triton X- in PBS for 5 min. The cells were blocked for 1 h at room temperature with 3% BSA with 0.05% Triton X-. The cells were incubated overnight at 4°C with primary antibodies for Myo1c (1:50 dilution)(Santa Cruz Biotechnology, sc-136544) and Jag1 (1:100 dilution) (Cell Signaling Technology, #2620). The cells were washed three times with PBS before incubating with Alexa 488 anti-rabbit secondary antibody (1:500), Alexa 555 anti-mouse secondary antibody (1:500), and DAPI (1:1000) at room temperature for 1 h in the dark. The cells were washed twice with PBS and kept in PBS with 0.1% sodium azide in the dark, at 4°C. Fluorescence imaging was performed using a confocal laser-scanning microscope (LSM880; Carl Zeiss).

siRNA knockdown and inhibitors

Knockdown of Myo1c was performed by transfecting 25 nM siRNAs into target cells using an RNAiMAX transfection protocol. To target Myo1c, 4 pooled siRNAs were transfected (L-015121-00; Dharmacon Reagents), and as control 4 pooled Non-Targeting siRNAs were transfected (D-00181010, Dharmacon Reagents). Cells were incubated for 4 h with the transfection mix and provided with fresh medium. For inhibition of Myo1c, samples were treated with 5 μM of pentachloropseudilin, with DMSO as vehicle control (PCLP; Aobious).

QUANTIFICATION AND STATISTICAL ANALYSIS

GO analysis

Gene enrichment analysis was conducted using g:Profiler, a web-based server (biit.cs.ut.ee/gprofiler/gost). The functional profiling of the enrichment results was carried out in g:Gost (version e101_e.g.,48_p14_baf17f0) using the g:SCS algorithm with the significance threshold of 0.05. The most relevant GO terms were filtered and visualized.[42]

Quantification of the videos and western blotting

ImageJ.[41]

Statistical analysis

Statistical analyses were performed using GraphPad (10.4.2 (633)). Quantifications of blot were compared with t-tests, or one-way ANOVA with pairwise comparison.